

Obstacle Filtering Algorithm for Control of an Autonomous Road Vehicle in Public Highway Traffic

Qian Wang
Clemson University
Greenville, SC, USA

Beshah Ayalew
Clemson University
Greenville, SC, USA

ABSTRACT

This paper presents an obstacle filtering algorithm that mimics human driver-like grouping of objects within a model predictive control scheme for an autonomous road vehicle. In the algorithm, a time to collision criteria is first used as risk assessment indicator to filter the potentially dangerous obstacle object vehicles in the proximity of the autonomously controlled vehicle. Then, the filtered object vehicles with overlapping elliptical collision areas put into groups. A hyper elliptical boundary is regenerated to define an extended collision area for the group. To minimize conservatism, the parameters for the tightest hyper ellipse are determined by solving an optimization problem. By excluding undesired local minimums for the planning problem, the grouping alleviates limitations that arise from the limited prediction horizons used in the model predictive control. The computational details of the proposed algorithm as well as its performance are illustrated using simulations of an autonomously controlled vehicle in public highway traffic scenarios involving multiple other vehicles.

1. INTRODUCTION

The adoption of autonomous vehicle technology has immense potential for enhancing the safety and efficiency of the transportation systems as well as for reducing energy consumption and environmental pollution. However, in-addition to the many regulatory and infrastructure issues that have yet to be fully addressed, technically, the motion planning and control of autonomous road vehicles in public traffic is not a fully solved problem. This is not only because of the nonlinear differential constraints of the vehicle dynamics, but also the requirement of handling uncertainties from the environment, such as avoiding other static and moving object/vehicles and obeying changing traffic signs/signals and lane marks, while satisfying other objectives, e.g. passenger desired speed and comfort or maximizing energy/fuel efficiency.

Most existing planning algorithms come from the robotics field, and apply approximations to simplify the planning problem. Specifically, those motion planning methods dealing with

differential constraints and obstacle avoidance can be roughly divided into three categories [1]: sampling-based methods, decoupling methods and mathematical programming methods. In the sampling-based method, the state space and input space of the autonomously controlled vehicle (ACV) can be deterministically discretized [2] or randomly sampled [3] in lattices from which the best collision free trajectories can be searched for. However, the existence and optimality of the solution depends on the size of the lattice, namely, they are guaranteed in resolution or probability [4]. And the computational time increases along with the lattice size. In decoupling methods, the planning problem is usually decomposed into two easier sub-problems [5]: first, applying a path planner (could be based on cell decomposition as in [6], or a sampling-based method) to find the waypoints in the configuration space, considering the shape of the ACV, and then using a close-loop controller to track those waypoints. The differential constraints are typically only applied to the latter sub-problem. Nevertheless, it's hard to prove the existence and the optimality of the collision-free solution, especially in the presence of uncertainties. Mathematical programming methods applies constrained numerical optimization to find the motion plan which guarantees a conditional existence and optimality of the solution based on the convexity of the problem formulation and the quality of the initial guess [7].

Model predictive control (MPC [8]), which belongs to the last group, is receiving significant attention in motion planning of ACVs perhaps since its finite receding horizon optimization scheme models human drivers very well [9]. Ref [10] has applied MPC for static obstacle avoidance and [11] has formulated it as a local reactive controller for trajectory planning to simultaneously track the path and avoid dynamic obstacles. In [12] [13], the motion planning and guidance of ACVs are formulated for general public traffic scenarios by adopting coordinate systems that treat lane centerlines as reference paths and uniformly expressing the motion of the controlled vehicle and all other objects, traffic rules/signs, lane limits, and road friction limits within the prediction horizon. The authors of the present paper have also extended the framework to the case of multi-lane scenarios by first structuring the controlled vehicle's maneuvers

in finite state machines which lead to a hybrid system framework, where rule-based [14] and optimal maneuver selections can be sought [15].

When formulating obstacle avoidance constraints for the prediction horizon, it is possible to model the dynamic motion of surrounding obstacle vehicles. However, to do this, one invariably needs to impose some assumptions about the unknown future inputs to these obstacle vehicles, inputs which are not generally available to the ACV controlled by MPC. However, by using the latest information about obstacles and the environment constructed from available sensing via radar, lidar, camera and V2V or V2I communications, one can minimize the required complexity of the models needed to describe the motions of the object vehicles. This can in turn help to reduce the computations of the MPC so that they can be completed fast enough and then take advantage of frequent updates. Using the MPC internal time as a state variable and the latest accelerations, speeds and positions of obstacle objects obtained by sensing or communication, one can derive algebraic descriptions of the motion of the geometries representing obstacle object vehicles for the whole prediction horizon [13].

There are several ways of modeling the geometric descriptions in the 2D configuration space [4], including e.g. polygonal models [16], described by the combination of linear curves; semi-algebraic models, like polynomials; or algebraic models like circles, ellipses [17] or hyper-ellipses [18]. Algebraic models are more efficient in describing obstacles with multi-edges since they generally need fewer parameters to be specified. For example, for describing a rectangular obstacle (4 edges), applying linear curves requires 8 parameters, while only 4 parameters are required for a conservative ellipse or hyper-ellipse. In our previous work [12] [14] [15], ellipses are used to describe the geometry of static/dynamic vehicular obstacles for MPC-based motion planning. It can be argued that ellipses naturally and conservatively describe the 2D geometry of modern road vehicles. However, possible overlaps in the prevailing distribution of the obstacles/ellipses may create undesirable local minima (or global minima for the finite horizon planning problem), which may trap the ACV. In addition, in the presence of more obstacle object vehicles around the ACV, the total number of evaluations for constraint violation/collision detection increases, which increases the complexity of, and the execution times needed for solving the optimization problem at each MPC update.

In this paper, we propose a concept of obstacle filtering concept and algorithm for the prediction of the motion of obstacle vehicle objects around an autonomous vehicle in public traffic. The algorithm may mimic human driver like cognitive actions [19] and covers three procedures: risk assessment, obstacle grouping and group boundary re-generation. This algorithm adaptively refines the constrain set to create a configuration space that excludes undesired local or global minima from possible overlaps of elliptic geometries, thus improving the performance of the MPC optimization solver in finding the best solution for the motion plans. The performance of the algorithm will be illustrated through a simulation of ACV in highway scenarios with several surrounding object (OVs).

The rest of the paper is organized as follows. Section 2 introduces the control framework. Section 3 details the obstacle filtering algorithm and Section 4 briefly reviews the configuration of the hybrid predictive trajectory guidance in which the filtering algorithm is to be embedded with. Simulation results are included in Section 5 to illustrate the workings of the proposed framework. Section 6 presents the conclusions of this contribution.

2. CONTROL FRAMEWORK

As mentioned above, the proposed obstacle filtering algorithm is incorporated into the obstacle motion prediction module of hybrid predictive control framework for autonomous vehicles that the authors presented earlier in [14], [15]. In the context of the present paper, the control framework is updated as shown in Fig. 1. Basically, it consists of five modules: environment recognition, route navigator, obstacle motion prediction, hybrid predictive trajectory guidance (HPTG) and vehicle dynamics control (VDC).

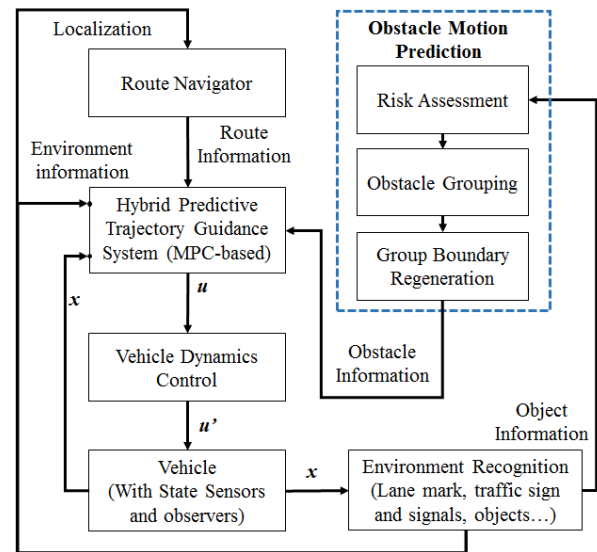


Figure 1. CONTROL FRAMEWORK

The environment recognition module captures the environment information, such as lane marks, traffic signs or signals, the size or states of moving objects, the state of the ACV and its localization through camera, radar, lidar or wireless devices. The route navigator module works as a general GPS navigator, which plans the route from initial position to target destination based via some algorithm on a map and localization of the controlled vehicle. In the following discussions, we assume all the information from environment recognition and route navigator are known to the guidance system.

The obstacle motion prediction module estimates the future motion of the obstacles and collision areas based on current measurements. Here, obstacles refers mostly to object vehicles (OVs) and they are all described by moving conservative ellipses

representing collision areas, in the configuration space. This module includes the three procedures of the object filtering algorithms: 1) Risk assessment, where the detected surrounding OV will be filtered by evaluating their risk of having collision with the autonomously controlled vehicle (ACV); 2) Obstacle grouping, where, based on their distances between each other, the filtered OVs will be grouped into different sub-lists that have intersecting collision areas; 3) Group boundary regeneration, where, the elliptical collision area of OVs in the same group will be covered by optimally parameterized hyper-elliptical boundary that includes all collision areas in the same group. Therefore, the obstacle motion prediction of the collision area for individual OVs will be transformed to OV groups. This reduces the difficulty of using large numbers of independent descriptions of OVs for collision avoidance constrains in the MPC formulation. Further details on the module will be given in the next section.

The HPTG module is responsible for the maneuver and trajectory planning of the ACV. A hierarchical planning structure is applied in this module: at the top, suite of finite state machines representing different maneuvers are selected, and at the bottom, a MPC-based trajectory planner computes the control references for the vehicle dynamics control level (VDC). The maneuver planning at the top can be either rule-based or optimization based. For rule-based maneuver planning, a maneuver will be selected based on pre-defined rules; while in the optimization-based maneuver planning, several pre-selected maneuvers will be sent to the MPC to solve for the optimal maneuver plans as well as the related trajectory plans. Interested readers are referred to [14] [15] for more detailed descriptions of the HPTG module. Details on the lower level VDC options can be found in [20].

3. Motion Prediction of Object Vehicles

To provide obstacle information for the MPC in the HPTG, the predicted motion of the OVs needs to be estimated by some motion model within the prediction horizon H_p , which is discretized with N_p samples; the time interval between two adjacent samples is Δt , thus $H_p = N_p \Delta t$. In this work, we adopt a simple kinematics model for the motion of objects using current measurements (assumed available from sensing or V2V/I communications). Considering a road frame s/y_e on a reference path, e.g. the center line of a lane, as shown in Fig. 1, the predicted longitudinal and lateral positions s_{o_i}, y_{e,o_i} of OV i can be defined by:

$$s_{o_i} = s_{o_i,0} + v_{t,o_i}^s t + \frac{1}{2} a_{t,o_i}^s t^2 \quad (1)$$

$$y_{e,o_i} = y_{e,o_i,0} + v_{n,o_i}^s t + \frac{1}{2} a_{n,o_i}^s t^2 \quad (2)$$

where, t is the time in the prediction model (which evolves the same as, and shares the re-set of the internal time defined in the MPC optimization). The position estimation is based on the current measurement of the longitudinal velocity v_{t,o_i}^s , longitudinal acceleration a_{t,o_i}^s , lateral velocity v_{n,o_i}^s and lateral

acceleration a_{n,o_i}^s . The acceleration components at the initial time(at MPC update/measurement) a_{t,o_i}^s and a_{n,o_i}^s are assumed constant for the prediction horizon. The initial positions of object i (at prediction) are denoted by $(s_{o_i,0}, y_{e,o_i,0})$.

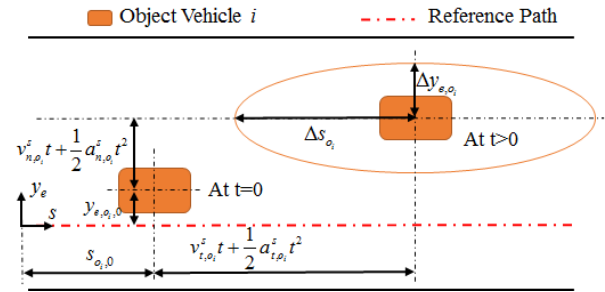


Figure 2. OBJECT VEHICLE MOTION DEFINITION IN ROAD REFERENCE FRAME

The related elliptical collision area for the ACV to avoid is described by

$$\left(\frac{y_{e,A} - y_{e,o_i}}{\Delta y_{e,o_i}} \right)^2 + \left(\frac{s_A - s_{o_i}}{\Delta s_{o_i}} \right)^2 \geq 1 \quad (3)$$

where $y_{e,A}, s_A$ are the longitudinal and lateral positions of the ACV in the road frame. $\Delta y_{e,o_i}$ and Δs_{o_i} are calculated by incorporating the geometry (length and width), velocity and the posture of the OVs and the ACV on the configuration space [12] [13].

3.1 Risk assessment

The risk here are associated with physical collision between the ACV and OVs, which is represented by the ACV entering the collision area defined around the OVs. Based on the kinematics model used to predict the motion of OVs, we use time to collision (TTC) T_c as an indicator to assess the risk of collision with in the detection range s_d , of the deployed sensors. Thus, we can define a range between ACV and OV i where a collision might happen along the reference path within a specified positive time T_c as:

$$|s_A - s_{o_i}| < s_d \quad (4)$$

$$0 < \frac{s_{o_i} - s_A}{v_{t,A}^s - v_{t,o_i}^s} < T_c \quad (5)$$

where $s_A, v_{t,A}^s$ are the longitudinal position and velocity of the ACV in the road frame. The OVs with their states satisfying both Eq. (4) and (5) will be considered to enough proximity to have potential danger of collision with the ACV, regardless of which lane they occupy.

3.2 Obstacle Grouping

In obstacle grouping, two step are followed. First, we need to determine if two OVs have intersecting collision areas. The sufficient condition for no overlapping of two ellipses with their axes (either major axes or minor axes) parallel to each other can

be easily derived. Second, this condition is applied to all the OV's filtered by the risk assessment step, to identify the groups and OV's belonging to each group.

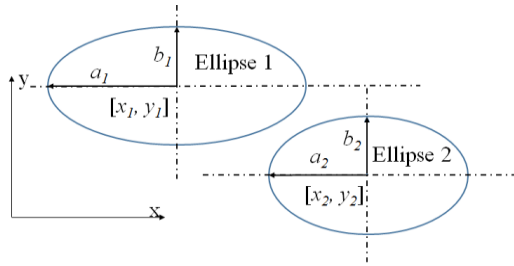


Figure 3. DEFINITION OF TWO ELLIPSES WITH THEIR AXES PARALLEL TO EACH OTHER

Any two ellipses with their axes parallel to each other, as shown in Fig. 3, can be defined by the following standard forms:

$$\left(\frac{x_{E1} - x_1}{a_1}\right)^2 + \left(\frac{y_{E1} - y_1}{b_1}\right)^2 = 1 \quad (6)$$

$$\left(\frac{x_{E2} - x_2}{a_2}\right)^2 + \left(\frac{y_{E2} - y_2}{b_2}\right)^2 = 1 \quad (7)$$

where $[x_{E1}, y_{E1}]$, $[x_{E2}, y_{E2}]$ are the points on the two ellipses. $[x_1, y_1]$, $[x_2, y_2]$ are the center of the two ellipses. a_1, a_2 are the half major axes of the two ellipses. b_1, b_2 represent the half minor axes of the two ellipses.

Starting with external tangentiality condition, it can be shown that the sufficient condition for two given ellipses to not overlap with each other is to simultaneously satisfy Eq.(8) and (9). See Appendix A for the derivation of these conditions.

$$\left(\frac{x_2 - x_1}{a_1 + \frac{a_2^2 b_1}{\min[a_1 b_2, a_2 b_1]}}\right)^2 + \left(\frac{y_2 - y_1}{b_1 + \frac{a_1 b_2^2}{\min[a_1 b_2, a_2 b_1]}}\right)^2 \geq 1 \quad (8)$$

$$\left(\frac{x_1 - x_2}{a_2 + \frac{a_1^2 b_2}{\min[a_1 b_2, a_2 b_1]}}\right)^2 + \left(\frac{y_1 - y_2}{b_2 + \frac{a_2 b_1^2}{\min[a_1 b_2, a_2 b_1]}}\right)^2 \geq 1 \quad (9)$$

Therefore, we can design a function J_o in Eq.(10) to identify the overlap condition of any two OV's i and j by comparing J_o with 2: if $J_o \geq 2$, the collision area of OV i and OV j don't overlap; if $J_o < 2$, the collision area of OV i and OV j overlap.

$$J_o = \left(\frac{s_{o,i} - s_{o,j}}{\Delta s_{o_i} + \frac{\Delta s_{o_i}^2 \Delta y_{e,o_j}}{\min[\Delta s_{o_i} \Delta y_{e,o_j}, \Delta s_{o_j} \Delta y_{e,o_i}]}}\right)^2 + \left(\frac{y_{e,i} - y_{e,j}}{\Delta y_{e,o_j} + \frac{\Delta s_{o_j} \Delta y_{e,o_i}^2}{\min[\Delta s_{o_i} \Delta y_{e,o_j}, \Delta s_{o_j} \Delta y_{e,o_i}]}}\right)^2 \quad (10)$$

$$+ \left(\frac{s_{o,j} - s_{o,i}}{\Delta s_{o_j} + \frac{\Delta s_{o_j}^2 \Delta y_{e,o_i}}{\min[\Delta s_{o_i} \Delta y_{e,o_j}, \Delta s_{o_j} \Delta y_{e,o_i}]}}\right)^2 + \left(\frac{y_{e,j} - y_{e,i}}{\Delta y_{e,o_i} + \frac{\Delta s_{o_i} \Delta y_{e,o_j}^2}{\min[\Delta s_{o_i} \Delta y_{e,o_j}, \Delta s_{o_j} \Delta y_{e,o_i}]}}\right)^2$$

Then, we can define the group by the following statement: A group consists of set of OV's where for anyone OV in the group, there is another OV with a collision area overlapping with it.

3.3 Group Boundary Regeneration

After identifying the OV groups, a new collision area can be regenerated for the group to cover the collision areas of all OV's in the group and systematically exclude the undesired local and global minimums that come from overlapping elliptical intersections (Fig.4). Here, we use the 4th order hyper ellipse to re-generate the boundary. This algebraic geometry requires few parameters to characterize and define a continuous boundary for the conservative collision area of the group. Below, we shall seek the tightest description of this boundary that doesn't waste too much collision free space.

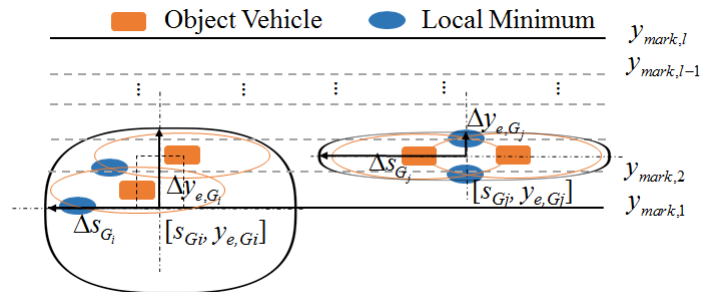


Figure 4. EXAMPLE OF 4TH ORDER HYPER ELLIPTICAL GROUP BOUNDARY REGENERATION

To being with, the 4th order hyper elliptical boundary for the ACV to avoid group i is defined as:

$$\left(\frac{y_{e,A} - y_{e,G_i}}{\Delta y_{e,G_i}}\right)^4 + \left(\frac{s_A - s_{G_i}}{\Delta s_{G_i}}\right)^4 \geq 1 \quad (11)$$

where s_{G_i}, y_{e,G_i} are the center position of the group i , which can be obtained by taking the average of the longitudinal and lateral positions of the constituent OV's in the group. However, the lateral position y_{e,G_i} , also depends on the positions of the element OV's. If one of the OV's is on the side lane next to the road boundary, y_{e,G_i} can be placed on the road boundary to guide the ACV to the available lanes on the other side of the road and to avoid creating local minimums at the intersections of the hyper elliptical boundary and the road boundary, as show in Fig. 4 (left).

$$s_{G_i} = \frac{1}{N_{G_i}} \sum_{n=1}^{N_{G_i}} s_{o_n} \quad (12)$$

$$y_{e,G_i} = \begin{cases} y_{mark,1}, & \text{if } \exists y_{e,o_n} \in [y_{mark,1}, y_{mark,2}], n \in \{1, 2, \dots, N_{G_i}\} \\ y_{mark,l}, & \text{if } \exists y_{e,o_n} \in [y_{mark,l-1}, y_{mark,l}], n \in \{1, 2, \dots, N_{G_i}\} \\ \frac{1}{n_o} \sum_{i=1}^{n_o} y_{c,ei}, & \text{else} \end{cases} \quad (13)$$

where N_{G_i} is the number of OV's in group i .

The half minor and half major axes $\Delta y_{e,G_i}$ and Δs_{G_i} of the tightest boundary of the group can be determined by posing an optimization problem. That is, we seek to find the hyper ellipse with minimum area that covers all the collision areas of the constituent OV's. As the area of a hyper ellipse is proportional to the product of the length of the major and minor axes, the optimization problem can be defined as:

$$\min_{\Delta s_{G_i}, \Delta y_{e,G_i}} \Delta s_{G_i} \Delta y_{e,G_i} \quad (14)$$

subject to:

$$\begin{cases} \left(\frac{s_{s,G_i} - s_{o_1}}{\Delta s_{o_1}} \right)^2 + \left(\frac{y_{e,s,G_i} - y_{e,o_1}}{\Delta y_{e,o_1}} \right)^2 \geq 1 \\ \vdots \\ \left(\frac{s_{s,G_i} - s_{o_{N_{G_i}}}}{\Delta s_{o_{N_{G_i}}}} \right)^2 + \left(\frac{y_{e,s,G_i} - y_{e,o_{N_{G_i}}}}{\Delta y_{e,o_{N_{G_i}}}} \right)^2 \geq 1 \end{cases} \quad (15)$$

where s_{s,G_i}, y_{e,s,G_i} are the position vectors including the longitudinal and lateral positions $[s_{s,G_i}, y_{e,s,G_i}]$ sampled from the boundary of the hyper ellipse by using the parametric equations of a 4th order hyper ellipse:

$$s_{s,G_i} = s_{G_i} + \Delta s_{G_i} \sqrt{|\cos \theta|} \operatorname{sgn}(\cos \theta) \quad (16)$$

$$y_{e,s,G_i} = y_{e,G_i} + \Delta y_{e,G_i} \sqrt{|\sin \theta|} \operatorname{sgn}(\sin \theta) \quad (17)$$

where θ is a parameter sampled from $-\pi$ to π .

This optimization problem can be solved efficiently if good initial guesses are given. Fig.5 shows the execution time for solving the optimization problem under different numbers of OV's located randomly and sampling points on the hyper ellipse. All the problems are solved via active-set sequential quadratic programming (SQP) method in MATLAB Optimization Toolbox running in a laptop with Intel i5 4200U CPU, 2.4GHz and 4G RAM. It can be seen that with more object vehicles and finer sampling of the hyper ellipse, the execution times can be substantial (order of 40ms with 10 OV's and 500 samples). Since this boundary regeneration step must be solved for each discretization step of the prediction horizon independently, the computations should ideally be done in parallel without adding to the execution time. This can be done on graphics processors which are likely available onboard ACVs for signal processing and object identification [21].

By following the three steps of the obstacle filtering

algorithm, and applying them to all discretization steps of the prediction horizon, the parameters defining the obstacle avoidance constraint can be determined for the whole horizon and sent to the HPTG module for motion planning.

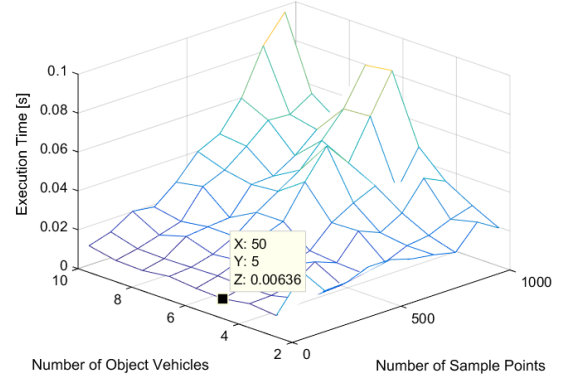


Figure 5. ESTIMATED EXECUTION TIMES FOR SOLVING THE OPTIMIZATION PROBLEM OF EQ.(14)

4. Hybrid Predictive Trajectory Guidance

We embed the above algorithm within the constraint formulations for the HPTG module described in our prior work [15]. The multi-objective optimization problem solved at each MPC update is:

$$\min_{x_k, u_k} \sum_{k=1}^{N_p} \sum_{q \in Q} \|Z_{q,k} (y_{1,k} - r_{1,q,k})\|_{P_1}^2 + \sum_{k=1}^{N_p} \|y_{2,k} - r_{2,k}\|_{P_2}^2 + \sum_{k=0}^{N_p-1} \|u_k\|_R^2 \quad (18)$$

$$\text{subject to: } \dot{x} = f(x, u), \quad u \in U, \quad x \in X \quad (19)$$

$$y_1 = A_1 x \quad (20)$$

$$y_2 = A_2 x \quad (21)$$

$$x(0) = x_0 \quad (22)$$

$$0 \leq c(x, u) \quad (23)$$

Here, x covers all the state variables of the planning model (ACV motion model, path and vehicle dynamics constraints) and slack variables for constraint adaptation and maneuver/lane selection. X represents the state space for x . Z_q is the maneuver selection variable with index q , included in the state in x and it should satisfy:

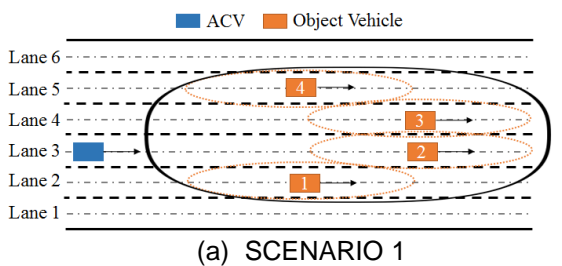
$$\sum_{q \in Q} Z_q = 1, \quad Z_q \in [0, 1] \quad (24)$$

Q is the maneuver set. x_0 denotes the current/initial state. $r_{1,q}, r_2$, are, respectively, the candidate references on different maneuvers and the slack variables. P_1, P_2 and R are the weighting matrices for the candidate maneuver tracking error, slack variable for reference tracking error and control efforts, respectively. y_1, y_2 are

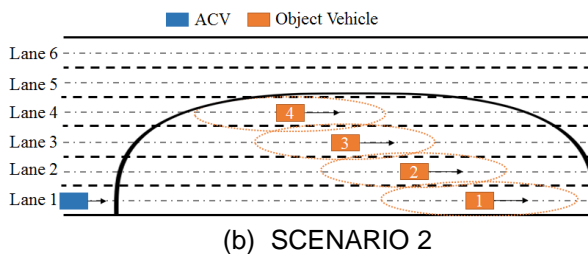
the system outputs, including the speed and lateral position of the ACV and the slack variables. The control vector u includes the longitudinal and lateral reference inputs to the lower level VDC. The control is treated as piecewise constant, as u_k , in the MPC optimization and only the first step u_1 will be applied to ACV before the next MPC update step. U denotes the admissible set for u . All the nonlinear constraints such as road-friction limits, as well as the individual OV collision avoidance constraints (3) and the group hyper ellipse (11) are included in the compact notation (23). Readers are referred to [15] for a more detailed description of the HPTG module.

5. Results and Discussion

In this section, we include some simulation results to illustrate the benefit of using the obstacle filtering algorithm when ACV faces complex traffic situations. For example, when a group of slower OVs in front of ACV creates an area, which leads to undesirable global minimums for the maneuver planning and local minimums for the trajectory planning.



(a) SCENARIO 1



(b) SCENARIO 2

Figure 6. HIGHWAY SCENARIO DESCRIPTION WITH SINGLE GROUP OF OVS

Firstly, two highway scenarios with six lanes and four OVs shown in Fig. 6a, b. are used for illustration. Scenario 1 happens in the middle of the roadway, while Scenario 2 happens near one side of the roadway. In both of these scenarios, the OVs are set to be running at the same constant speed at 25m/s that is lower than the desired cruise speed of the ACV at 30m/s. When obstacle filtering algorithm is applied, the overlapped elliptical collision boundary will be replaced by an extended hyper elliptical boundary with parameters calculated using Eqs. (12)-(14). Otherwise, the original elliptical collision area for each individual OV will be used for obstacle avoidance.

To clearly show the relative positions between the OV and the ACV in the configuration space, we use the relative path profile, which describes the positions in a moving coordinate

$\Delta s/y_e$ at the same speed along the reference path as the OVs. Thus the OVs will be static in this coordinate but the path profile of the ACV and its planned path, if at differing speeds, will be described by curves in the coordinate.

Fig.7 and 8 show the results of the ACV in Scenario 1 with and without applying the obstacle filtering algorithm. We can see in the case with obstacle filtering, ACV initially plans to slow down when it detects OV 2 in front. When it approaches the hyper elliptical boundary, it plans to change lane to the right to avoid the group of OVs. As this boundary moves with the group of OVs, smooth trajectories are planned during the obstacle avoidance. While in the case w/o obstacle filtering, it plans to slow down to follow OV 2 (a global minimum for maneuver planning) and the ACV can't maintain or return to its desired cruise speed.

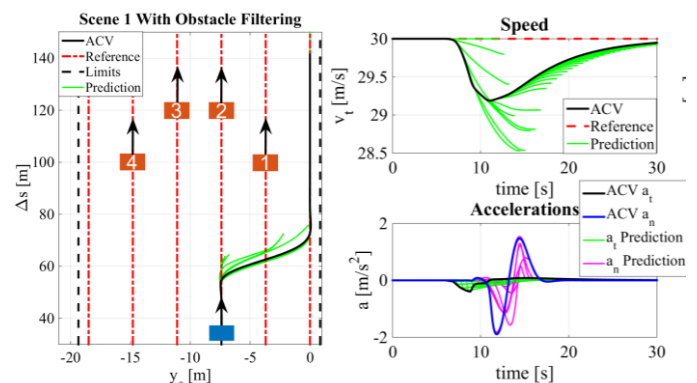


Figure 7. RESULTS FOR SCENARIO 1 WITH OBSTACLE FILTERING

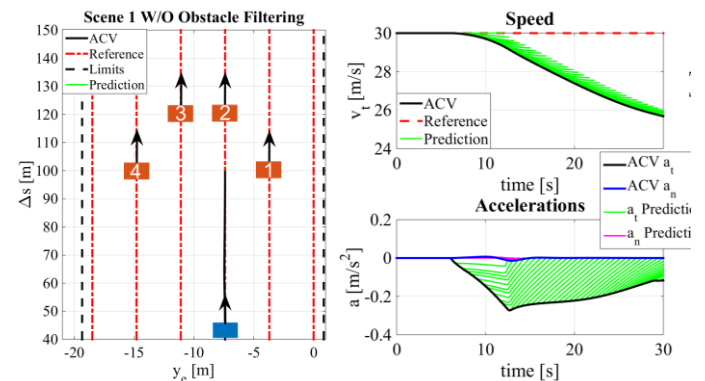


Figure 8. RESULTS FOR SCENARIO 1 WITHOUT OBSTACLE FILTERING

Fig.9,10 shows the results of ACV in Scenario 2 with and without applying the obstacle filtering algorithm. In the former case, ACV initially plans to slow down when it approaches the hyper elliptical boundary. Then, it plans to change lane to the lane 5 at the left to avoid the group of OVs, while increasing its speed to track the reference. However, in the case w/o obstacle filtering, it plans to slow down first and then change lane to the left. But the left lane is also occupied by OV2, thus the ACV moves back to lane 1 and finally follows the slower OV 1, which is also an

undesirable global minimum for maneuver planning.

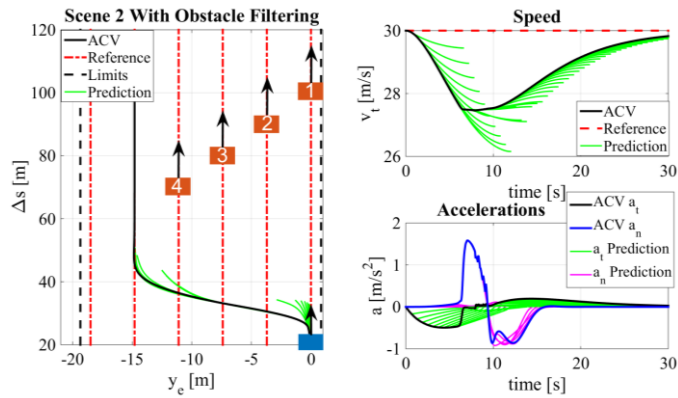


Figure 9. RESULTS FOR SCENARIO 2 WITH OBSTACLE FILTERING

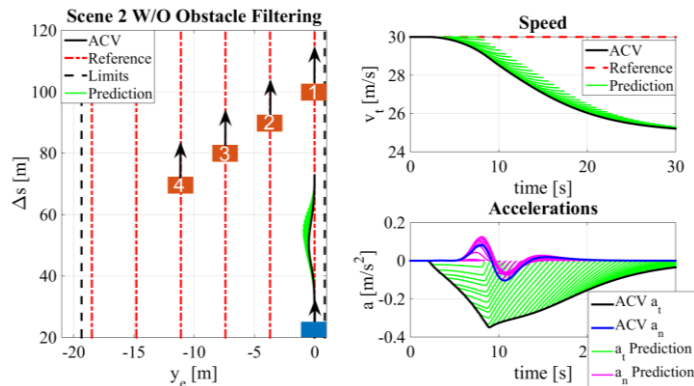


Figure 10. RESULTS FOR SCENARIO 2 WITHOUT OBSTACLE FILTERING

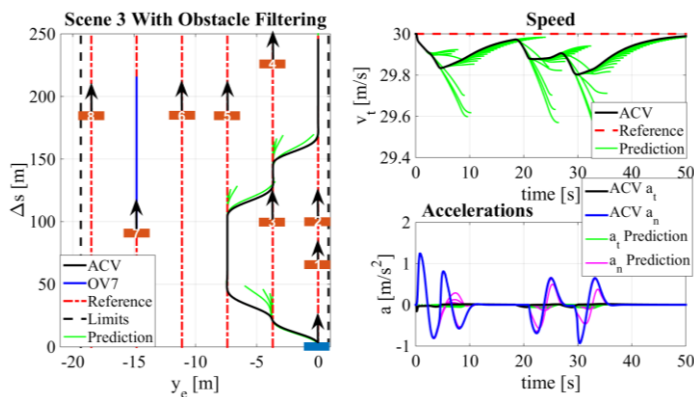


Figure 11. RESULTS FOR SCENARIO 3 WITH OBSTACLE FILTERING

Finally, a highway scenario 3 with 8 OVs shows the results for multiple OVs grouping and the dynamic change of the group boundary, as depicted in Fig. 11. Here, all of the OVs are running at 25m/s except for OV7, which is at speed of 27.5m/s. OV1, 2 and 3 present the first group that ACV will face. When ACV passes the first group by changing lane to lane 3, as OV7 is

approaching the group of OV5 and 6, it also connect OV6 with OV8, thus the original group OV5 and 6 will be extended to a bigger group including from OV5 to OV8. This group change is consider by the HPTG in the prediction horizon and it guides the ACV to change back to lane 2 to avoid the new group. Finally ACV changes lane to lane 1 to pass the single OV4.

6. CONCLUSION

In this paper, we proposed an obstacle filtering algorithm to pre-processes the obstacle information for the hybrid predictive control of autonomous road vehicle in public traffic. The algorithm has the following steps. First, Time to Collision is used as risk assessment indicator to filter the potentially dangerous object vehicles (OV) around the autonomously controlled vehicle (ACV). Then different OV groups are created for OVs with overlapping elliptical collision areas. Finally, the boundary of the group will be described by a 4th order hyper ellipse to define an extended collision area which covers all the independent collision areas of the OVs inside the group. This helps to exclude the undesired global minimums or local minimums, thus simplifies the planning problem by changing the configuration space. The performance of the collaborated control system is illustrated via the simulations on highway scenarios to avoid a group of OVs.

REFERENCE

- [1] C. Goerzen, Z. Kong and B. Mettler, "A Survey of Motion Planning Algorithms from the Perspective of Autonomous UAV Guidance," *Journal of Intelligent and Robotic Systems*, vol. 57, no. 1-4, pp. 65-100, 2010.
- [2] A. Liniger and J. Lygeros, "A viability approach for fast recursive feasible finite horizon path planning of autonomous RC cars," in *Proceedings of the 18th International Conference on Hybrid Systems: Computation and Control*, Seattle, Washington, USA, 2015.
- [3] E. Frazzoli, M. Dahleh and E. Feron, "Real-time motion planning for agile autonomous vehicles," in *American Control Conference*, Arlington, VA, USA, 2001.
- [4] S. M. LaValle, *Planning Algorithms*, Cambridge University Press, 2006.
- [5] K. Kant and S. W. Zucker, "Toward efficient trajectory planning: The path-velocity decomposition," *The International Journal of Robotics Research*, vol. 5, no. 3, pp. 72-89, 1986.
- [6] D. Ferguson, M. Likhachev and A. Stentz, "A guide to heuristic-based path planning," in *Proceedings of the international workshop on planning under uncertainty for autonomous systems, international conference on automated planning and scheduling (ICAPS)*, 2005.
- [7] S. Boyd and L. Vandenberghe, *Convex optimization*, Cambridge university press, 2004.

- [8] J. Maciejowski, Predictive Control: With Constraints, Harlow, UK: Prentice-Hall, 2002.
- [9] G. Prokop, "Modeling human vehicle driving by model predictive online optimization," *Vehicle System Dynamics*, vol. 35, no. 1, pp. 19-53, 2001.
- [10] J. Liu, P. Jayakumar, J. L. Stein and T. Ersal, "An MPC Algorithm with Combined Speed and Steering Control for Obstacle Avoidance in Autonomous Ground Vehicles," in *ASME 2015 Dynamic Systems and Control Conference*, Columbus, OH, 2015.
- [11] Y. Gao, T. Lin, F. Borrelli, E. Tseng and D. Hrovat, "Predictive control of autonomous ground vehicles with obstacle avoidance on slippery roads," in *ASME 2010 Dynamic Systems and Control Conference*, Cambridge, Massachusetts, 2010.
- [12] T. Weiskircher and B. Ayalew, "Predictive Control for Autonomous Driving in Dynamic Public Traffic," in *American Control Conference*, Chicago, IL, 2015.
- [13] T. Weiskircher, Q. Wang and B. Ayalew, "A Predictive Guidance and Control Framework for (Semi-)Autonomous Vehicles in Public Traffic," *IEEE Transactions on control systems technology*. (Under Review)
- [14] Q. Wang, T. Weiskircher and B. Ayalew, "A Hierarchical Hybrid Predictive Control of an Autonomous Vehicle," in *ASME 2015 Dynamic System and Control Conference*, Columbus, Ohio, USA, 2015.
- [15] Q. Wang, B. Ayalew and T. Weiskircher, "Optimal Assigner Decisions in Predictive Control of an Autonomous Road Vehicle," in *American Control Conference*, Boston, MA, USA, 2016.
- [16] J. Nilsson, P. Falcone, M. Ali and J. Sjöberg, "Receding horizon maneuver generation for automated highway driving," *Control Engineering Practice*, vol. 41, pp. 124-133, 2015.
- [17] U. Rosolia, F. Braghin, A. Alleyne and E. Sabbioni, "NLMPC for Real Time Path Following and Collision Avoidance," *SAE International Journal of Passenger Cars-Electronic and Electrical Systems*, vol. 8, no. 2, pp. 401-405, 2015.
- [18] M. S. Menon and A. Ghosal, "Obstacle avoidance for hyper-redundant snake robots and one dimensional flexible bodies using optimization," in *14th World Congress in Mechanism and Machine Science*, Taipei, Taiwan, 2015.
- [19] D. D. Salvucci, "Modeling driver behavior in a cognitive architecture," *The Journal of the Human Factors and Ergonomics Society*, vol. 48, no. 2, pp. 362-380, 2006.
- [20] T. Weiskircher and B. Ayalew, "Frameworks for Interfacing Trajectory Tracking with Predictive Trajectory Planning for Autonomous Road Vehicle Control," in *American Control Conference*, Chicago, IL, USA, 2015.
- [21] Y. Cao, A. Seth and C. D. Laird, "An augmented Lagrangian interior-point approach for large-scale NLP problems on graphics processing units," *Computers & Chemical Engineering*, vol. 85, pp. 76-83, 2016.

ANNEX A

PROOF OF THE SUFFICIENT CONDITION FOR NON-OVERLAPPING OF TWO ELLIPSES WITH AXLES PARALLEL TO EACH OTHER

Use the parametric equation to describe the position of the ellipse defined in in Eq. (6),(7), we obtain:

$$\begin{cases} x_{E1} = x_1 + a_1 \cos \theta_1 \\ y_{E1} = y_1 + b_1 \sin \theta_1 \end{cases} \quad (25)$$

$$\begin{cases} x_{E2} = x_2 + a_2 \cos \theta_2 \\ y_{E2} = y_2 + b_2 \sin \theta_2 \end{cases} \quad (26)$$

Considering the externally tangential condition of the two ellipses defined in Eq. (25),(26), as shown in Fig. 11, the position of the intersection between the two ellipses at the common tangent should satisfied:

$$\frac{-b_1}{a_1} \cot \theta_1 = \frac{-b_2}{a_2} \cot \theta_2 \quad (27)$$

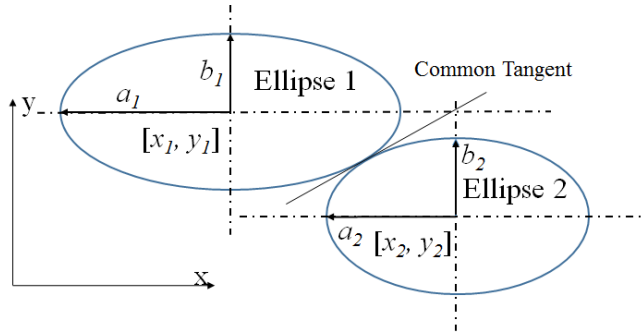


Figure 11. EXTERNAL TANGENCY OF THE TWO ELLIPSES

Assume ellipse 1 is fixed, combining Eq.(25)-(26), the algebraic equation for the center of ellipse 2 that externally tangential to the ellipse 1 can be derived by:

$$\begin{cases} x_2 = x_1 + \left(a_1 + \frac{a_2^2 b_1}{\sqrt{a_2^2 b_1^2 \cos^2 \theta_1 + a_1^2 b_2^2 \sin^2 \theta_1}} \right) \cos \theta_1 \\ y_2 = y_1 + \left(b_1 + \frac{a_1 b_2^2}{\sqrt{a_2^2 b_1^2 \cos^2 \theta_1 + a_1^2 b_2^2 \sin^2 \theta_1}} \right) \sin \theta_1 \end{cases} \quad (28)$$

which is bounded by

$$\begin{cases} \bar{x}_2 = x_1 + \left(a_1 + \frac{a_2^2 b_1}{\min[a_1 b_2, a_2 b_1]} \right) \cos \theta_1 \\ \bar{y}_2 = y_1 + \left(b_1 + \frac{a_1 b_2^2}{\min[a_1 b_2, a_2 b_1]} \right) \sin \theta_1 \end{cases} \quad (29)$$

Thus the sufficient condition for the split of ellipse 2 from ellipse 1 can be defined by:

$$\left(\frac{x_2 - x_1}{a_1 + \frac{a_2^2 b_1}{\min[a_1 b_2, a_2 b_1]}} \right)^2 + \left(\frac{y_2 - y_1}{b_1 + \frac{a_1 b_2^2}{\min[a_1 b_2, a_2 b_1]}} \right)^2 \geq 1 \quad (30)$$

Similarly, if ellipse 2 is fixed, the sufficient condition for the split of ellipse 1 from ellipse 2 can be defined by:

$$\left(\frac{x_1 - x_2}{a_2 + \frac{a_1^2 b_2}{\min[a_1 b_2, a_2 b_1]}} \right)^2 + \left(\frac{y_1 - y_2}{b_2 + \frac{a_2 b_1^2}{\min[a_1 b_2, a_2 b_1]}} \right)^2 \geq 1 \quad (31)$$

Therefore, simultaneously satisfying Eq. (30) and (31) guarantees the non-overlap of the two ellipses with parallel axes.